Inorg. Chem. **2003**, *42*, 2470−2477

Fe(II) and Fe(III) Mononuclear Complexes with a Pentadentate Ligand Built on the 1,3-Diaminopropane Unit. Structures and Spectroscopic and Electrochemical Properties. Reaction with H_2O_2

Véronique Balland,[†] Frédéric Banse,*[,†] Elodie Anxolabéhère-Mallart,*[,†] Morten Ghiladi,[†] Tony A. Mattioli,[‡] Christian Philouze,[§] Geneviève Blondin,[†] and Jean-Jacques Girerd*[,†]

Laboratoire de Chimie Inorganique, UMR CNRS 8613, Université Paris-Sud, 91405 Orsay, France, Laboratoire de Biophysique du Stress Oxydant, SBE/DBJC CEA/Saclay, 91191 Gif-sur-Yvette, France, and Laboratoire d'Etudes Dynamiques et Structurales de la Sélectivité, UMR 5616, 38041 Grenoble, France

Received July 26, 2002

Two new iron complexes, $[L_5{}^3Fe^{II}Cl]PF_6$ (**1**·PF_6) and $[(L_5{}^3H^+)Fe^{III}Cl_3]PF_6$ (**2**·PF_6), were synthesized ($L_5{}^3$ = *N*-methyl-*N*,*N*′,*N*′-tris(2-pyridylmethyl)propane-1,3-diamine), and their molecular structures were determined by X-ray crystallography. Their behavior in solution was studied by UV−vis spectroscopy and electrochemistry. Upon addition of a base to an acetonitrile solution of **2**, the new unsymmetrical dinuclear complex $[L_5{}^3Fe^{III}OFe^{III}Cl_3]^+$ was detected. Treating **1** with hydrogen peroxide has allowed us to detect the low spin $[L_5{}^3Fe^{III}OOH]^{2+}$. Its spectroscopic properties (UV−vis, EPR and resonance Raman) are similar to those reported for related FeOOH complexes obtained with amine/pyridine ligands. Using stopped-flow absorption spectroscopy, the formation and degradation of $[L_5{}^3Fe^{III}$-$OOH]^{2+}$ has been monitored, and a mechanism is proposed to reproduce the kinetic data.

Introduction

Pentadentate ligands have been successfully used to obtain Fe(III)−OOH species.[1] These species are synthetic models for the key enzymatic intermediates that form between the initial Fe^{II}−dioxygen adduct and the active form in the catalytic cycle of monoiron biomolecules capable of oxidative transformation, such as metabolism of medicines by cytochromes P450,[2,3] or DNA oxidative cleavage by bleomycin.[4]

In non-heme chemical systems, Fe(III)−OOH complexes are generally obtained by reaction of an excess of H_2O_2 with the corresponding Fe(II) complexes. The mechanism of this reaction is still unclear. It has also been shown that by adding a base it is possible to obtain the deprotonated Fe(III)O_2 form which appears to be of a side-on configuration.[5] The Fe(III)−OOH species are usually low spin except in one case reported by Wada et al.,[6] while the deprotonated Fe(III)O_2 species are usually high spin.[1] They can be used as spectroscopic models for non-heme iron enzymes interacting with O_2 as recently reported by Mathé et al.[7] Recently, the group of Kovacs, using a pentadentate ligand containing a thiolate group, has shown the formation of a peroxo species by the alternative route of reaction of superoxide with an Fe(II) complex.[8]

In the past, we and others have prepared Fe(III)−OOH and Fe(III)O_2 complexes using pentadentate ligands based on the 1,2-diaminoethane unit as L_5.[9−13] Owing to their relative stability, these complexes have been studied by different techniques (UV−vis, EPR, mass spectrometry,

* To whom correspondence should be addressed. E-mail: fredbanse@icmo.u-psud.fr (F.B.); eanxolab@icmo.u-psud.fr (E.A.-M.); jjgirerd@icmo.u-psud.fr (J.-J.G.).
[†] Laboratoire de Chimie Inorganique.
[‡] Laboratoire de Biophysique du Stress Oxydant.
[§] Laboratoire d'Etudes Dynamiques et Structurales de la Sélectivité.

(1) Girerd, J. J.; Banse, F.; Simaan, A. J. *Struct. Bond.* **2000**, *97*, 146−177.
(2) Sono, M.; Roach, M. P.; Coulter, E. D.; Dawson, J. H. *Chem. Rev.* **1996**, *96*, 2841.
(3) Benson, D. E.; Suslick, K. S.; Sligar, S. G. *Biochemistry* **1997**, *36*, 5104.
(4) Que, L.; Ho, R. Y. N. *Chem. Rev.* **1996**, *96*, 2607.
(5) Ho, R. Y. N.; Roelfes, G.; Hermant, R.; Hage, R.; Feringa, B. L.; Que, L. *Chem. Commun.* **1999**, 2161−2162.
(6) Wada, H.; Ogo, S.; Nagatomo, S.; Kitagawa, T.; Watanabe, Y.; Jitsukawa, K.; Masuda, H. *Inorg. Chem.* **2002**, *41*, 616−618.
(7) Mathé, C.; Mattioli, T. A.; Horner, O.; Lombard, M.; Fontecave, M.; Nivière, V. *J. Am. Chem. Soc.* **2002**, *124*, 4966−4967.
(8) Shearer, J.; Scarrow, R. C.; Kovacs, J. A. *J. Am. Chem. Soc.* **2002**, *124*, 11709−11717.
(9) Bernal, I.; Jensen, I. M.; Jensen, K. B.; McKenzie, C. J.; Toftlund, H.; Tuchagues, J. P. *J. Chem. Soc., Dalton Trans.* **1995**, 3667−3675.

10.1021/ic025905n CCC: $25.00
Published on Web 03/12/2003

resonance Raman, Mössbauer). A kinetic study has also been recently reported for the formation of an Fe(III)−OOH complex with a ligand of the L_5 family.[14]

In this paper, we study how the modification of the 1,2-diaminoethane central unit into a 1,3-diaminopropane one (by using L_5^3 instead of L_5) influences this type of chemistry. We found that this modification diminishes considerably the stability of the Fe(III)−OOH species although we can still detect it, in particular by stopped-flow spectrometry. This particularity has allowed us to monitor the formation and degradation of $[L_5^3Fe^{III}OOH]^{2+}$ and to propose a kinetic model.

Experimental Section

General Methods. All manipulations were carried out by using standard Schlenk techniques. Starting materials were purchased from Acros. Solvents were purchased from Merck and used without further purification except for electrochemistry experiments.

Electronic absorption spectra were recorded using a Varian Cary 5E spectrophotometer. For low-temperature measurements, a Dewar equipped with quartz windows was used. EPR spectra were recorded using an X-band Bruker ESP 300 E. Cyclic voltammograms (CVs) were measured using an EGG PAR model M270 scanning potentiostat operating at a scan rate of 10−1000 mV s^{-1}. Studies were carried out, under argon, in acetonitrile or methanol solutions using 0.2 M $^tBu_4NClO_4$ (Fluka) as the supporting electrolyte, and 10^{-3} M of the complex. The working electrode was a glassy carbon disk (0.32 cm^2) polished with 1 μm polishing powder. The reference electrode was Ag−$AgClO_4$ separated from the test solution by a salt bridge containing the solvent/supporting electrolyte, with gold as the auxiliary electrode. All potentials are given versus the SCE electrode. Controlled potential electrolyses were performed using the same equipment as the CV, except for the working electrode (platinum) and auxiliary electrode (platinum). Resonance Raman spectra were recorded using a Jobin Yvon spectrometer equipped with a 900 lines/mn gratings and a liquid-nitrogen cooled CCD camera. The 647.1 nm line of a Kr^+ laser was used for excitation with a power of 50 mW. The spectrometer was equipped with a Dewar with quartz windows for low temperatures (−50 °C), and concentration of the solution was 1.5 mM in iron. Under those conditions, the intermediate was stable for ca. 30 min. FT-IR spectra were recorded on a Perkin-Elmer Spectrum1000. For crystallographic data collection, the crystals of complex **1**·PF_6·methanol were mounted on an Enraf-Nonius CAD4 diffractometer whereas those of **2**·PF_6 were mounted on an Enraf-Nonius MACH3 diffractometer. Both diffractometers were equipped with graphite plate monochromators (λ(Mo Kα) = 0.71073 Å), and were run at 293 K. The reflections were corrected for Lorentz and polarization effects but not for absorption. Each structure was solved by direct methods and refined using TEXSAN software.[15]

Table 1. Summary of X-ray Crystallographic Data for **1**·PF_6·methanol and **2**·PF_6

	$[L_5^3Fe^{II}Cl]PF_6$-$(CH_3OH)_{0.85}$ **1**·PF_6·methanol	$[(L_5^3H^+)Fe^{III}$-$Cl_3]PF_6$ **2**·PF_6
empirical formula	$C_{22.85}H_{30.4}N_5O_{0.85}$-$FeClPF_6$	$C_{22}H_{28}N_5$-$FeClPF_6$
fw (g mol^{-1})	624.99	669.67
cryst syst	orthorhombic	triclinic
space group	*Pbca*	$P\bar{1}$
a (Å)	16.730(7)	8.824(3)
b (Å)	17.060(5)	12.140(4)
c (Å)	19.333(15)	15.089(4)
α (deg)	90	111.34(3)
β (deg)	90	97.76(3)
γ (deg)	90	101.63(3)
V ($Å^3$)/Z	5517(4)/8	1435(1)/2
D_x (g cm^{-3})	1.50	1.55
μ (cm^{-1})	7.67	9.20
cryst size (mm^3)	0.20 × 0.18 × 0.05	0.22 × 0.18 × 0.10
shape/color	platelet/reddish brown	prism/reddish brown
T (K)	293	293
$2\theta_{max}$ (deg)	56	60
no. reflns collected	7301	8630
no. unique reflns	7301	8334
no. reflns used	3629 [$F > 1.2\sigma(F)$]	3432 [$F > 1.6\sigma(F)$]
no. params refined	361	343
$R(F)^a$	0.0627	0.078
$R_w(F)^b$	0.0608	0.052
fudge factor, *p*	3.4×10^{-4}	7.2×10^{-5}
GOF, *S*	1.83	1.97
Dr_{min}/Dr_{max} (e $Å^{-3}$)	−0.383/0.494	−0.613/0.789

^{a} $R = \sum||F_o| - |F_c||/\sum|F_o|$. ^{b} $R_w = [\sum(|F_o| - |F_c|)^2/wF_o^2]^{1/2}$ with $w = 1/[\sigma^2(F_o) + p|F_o|^2]$.

The disorder within the PF_6 anion in **1**·PF_6·methanol was treated by splitting F5 and F6 on two different sites, and then, the population of each site was refined, then rounded off, and fixed to the closest value allowing a sum equal to 1. In **1**·PF_6·methanol, the methanol molecule had its population first refined, then rounded off, and fixed. All non-hydrogen atoms were refined with anisotropic thermal parameters. Hydrogen atoms were generated in idealized positions, riding on the carrier atoms, with isotropic thermal parameters, except for the hydrogen atoms of the methanol molecule, which were localized on difference Fourier map and then idealized.

In **2**·PF_6, all non-hydrogen atoms were refined with anisotropic thermal parameters. Hydrogen atoms were generated in idealized positions, riding on the carrier atoms, with isotropic thermal parameters, except for the hydrogen atom on the uncomplexed nitrogen atom of the amino group which was localized on difference Fourier map and then idealized. Further data collection parameters are listed in Table 1.

Synthesis of *N*-Methyl-*N*,*N*′,*N*′-tris(2-pyridylmethyl)propane-1,3-diamine (L_5^3). The ligand was synthesized as *N*-methyl-*N*,*N*′,*N*′-tris(2-pyridylmethyl)ethane-1,2-diamine using *N*-methylpropane-1,3-diamine as starting material.[9] The crude product obtained after evaporation of $CHCl_3$ was a dark oil purified by chromatography on Al_2O_3 (eluant $CHCl_3$/EtOH 20:1).

Synthesis of $[L_5^3Fe^{II}Cl]PF_6$ (1·PF_6). The ligand L_5^3 (300 mg; 0.83 mmol) was dissolved in methanol (5 mL) and added under Ar to a 5 mL methanol solution of $FeCl_2$·$2H_2O$ (132 mg, 0.81 mmol). The yellow solution was stirred under Ar for 1 h, and $NaPF_6$ (120 mg, 0.71 mmol) in methanol was added. The mixture was

(10) Mialane, P.; Novorojkine, A.; Pratviel, G.; Azéma, L.; Slany, M.; Godde, F.; Simaan, A.; Banse, F.; Kargar-Grisel, T.; Bouchoux, G.; Sainton, J.; Horner, O.; Guilhem, J.; Tchertanova, L.; Meunier, B.; Girerd, J. J. *Inorg. Chem.* **1999**, *38*, 1085−1092.
(11) Simaan, A. J.; Banse, F.; Mialane, P.; Boussac, A.; Un, S.; Kargar-Grisel, T.; Bouchoux, G.; Girerd, J. J. *Eur. J. Inorg. Chem.* **1999**, 993−996.
(12) Jensen, K. B.; McKenzie, C. J.; Nielsen, L. P.; Pedersen, J. Z.; Svendsen, H. M. *Chem. Commun.* **1999**, 1313−1314.
(13) Simaan, A. J.; Banse, F.; Girerd, J. J.; Wieghardt, K.; Bill, E. *Inorg. Chem.* **2001**, *40*, 6538−6540.
(14) Hazell, A.; McKenzie, C. J.; Nielsen, L. P.; Schindler, S.; Weitzer, M. *J. Chem. Soc., Dalton Trans.* **2002**, 310−317.
(15) *TEXSAN. Single-Crystal Structure Analysis Software*, Version 1.7; MSC, Molecular Structure Corporation: The Woodlands, TX, 1992−1997.

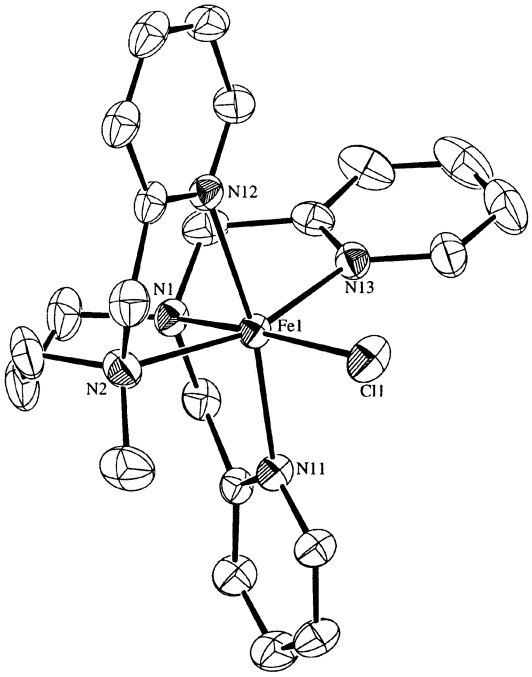

Figure 1. ORTEP view of the complex cation $[L_5{}^3Fe^{II}Cl]^+$ (**1**) with displacement ellipsoids shown at the 25% probability level. H atoms have been omitted for clarity.

concentrated and filtered, and 195 mg of pale yellow powder was obtained (yield 90%). Evaporation of a methanol−acetone solution of the powder yielded yellow crystals suitable for X-ray diffraction analysis. Elemental analysis found: C, 42.3; H, 4.38; N, 10.95. $C_{22}H_{27}N_5FeClPF_6$ requires: C, 44.21; H, 4.55; N, 11.72. FT-IR $\nu(cm^{-1})$: 1720, 1603, 1433, 1294, 838, 557.

Synthesis of $[(L_5{}^3H^+)Fe^{III}Cl_3]PF_6$ (2·PF_6). $L_5{}^3$ (185 mg, 0.51 mmol) in 2 mL of acetone was added to a 5 mL methanol solution of $FeCl_3{\cdot}6H_2O$ (270 mg, 1 mmol). The dark red solution was stirred for 1 h, and $NaPF_6$ (170 mg, 1 mmol) in methanol was added. The solution was stirred for 30 min and left to crystallize. Dark yellow crystals (290 mg) were obtained after a few days (yield 85% vs $L_5{}^3$). Elemental analysis found: C, 39.2; H, 4.2; N, 10.3. $C_{22}H_{25}N_5FeCl_3PF_6$ requires: C, 39.52; H, 4.22; N, 10.48. IR $\nu(cm^{-1})$: 3049, 1607, 1443, 1318, 842, 769, 558.

Results and Discussion

X-ray Crystal Structures. Single crystals of **1**·PF_6·methanol and **2**·PF_6 were isolated. The molecular structures of monocationic complexes **1** and **2** are shown in Figures 1 and 2, respectively. The iron ion in complex **1** is in a pseudo-octahedral environment, consisting of the five nitrogen atoms of the ligand and one chloride. The structure of the analogous complex $[L_5Fe^{II}Cl]^+$ with the ligand L_5 built on the 1,2-diaminoethane fragment has been previously described.[10] The comparison of selected bond distances and angles for these two related complexes is given in Table 2.

For both complexes, the mean value of the Fe−N distances is approximately 2.2 Å which is indicative of high spin Fe(II).[16] The octahedral geometry is less distorted for complex **1**. Indeed, angles around Fe(II) are closer to 90° except those

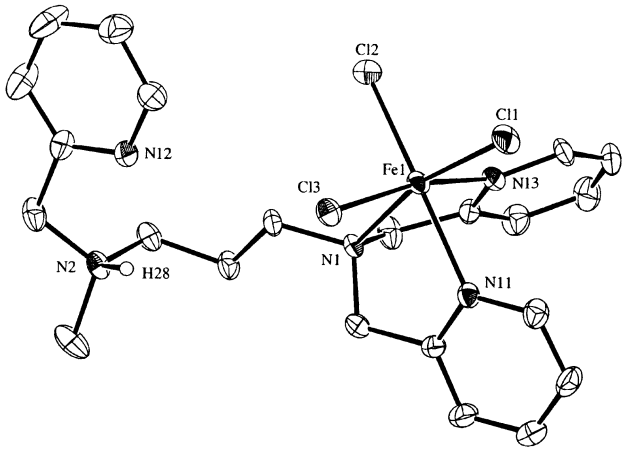

Figure 2. ORTEP view of the complex cation $[(L_5{}^3H^+)Fe^{III}Cl_3]^+$ (**2**) with displacement ellipsoids shown at the 25% probability level. H atoms have been omitted for clarity.

Table 2. Comparison of Selected Bond Distances (Å) and Bond Angles (deg) for Complexes $[L_5Fe^{II}Cl]^+$[a] and $[L_5{}^3Fe^{II}Cl]^+$

	$[L_5{}^3Fe^{II}Cl]^+$	$[L_5Fe^{II}Cl]^+$
$Fe-N_{13}$ (py)	2.1703	2.171
$Fe-N_{11}$ (py)	2.2084	2.270
$Fe-N_1$ (am)	2.2716	2.274
$Fe-N_2$ (am)	2.2627	2.248
$Fe-N_{12}$ (py)	2.1731	2.200
Fe−Cl	2.3718	2.330
$N_2-Fe-Cl$	96.139	104.51
$N_{13}-Fe-Cl$	96.914	106.79
N_1-Fe-N_2	94.218	78.36
N_1-Fe-N_{13}	74.506	74.05
N_2-Fe-N_{12}	77.772	74.32
N_1-Fe-N_{11}	75.559	75.67

[a] From ref 2.

belonging to a five-membered metallocycle, which remain close to 75° (N_1FeN_{11}, N_2FeN_{12}, N_1FeN_{13}). From L_5 to $L_5{}^3$, the introduction of a methylene group transforms the five-membered metallocycle N_1FeN_2 in a six-membered one, allowing the angle around Fe to go from 78.389° to 94.218°.

The structure obtained for complex **2** is somewhat unusual. It reveals the protonation of one amino nitrogen of the ligand. Therefore, the iron center is ligated by only three nitrogen atoms of the ligand in a facial configuration, and the pseudo-octahedral coordination sphere is completed by three chloride ions. As for complex **1**, Fe−N(py) distances (2.158 and 2.211 Å) are shorter than the Fe−N(amine) distance (2.265 Å). These distances are indicative of the high spin state of Fe(III) and are 0.2 Å longer than in low spin Fe(III), for instance in $[(TPEN)Fe]^{3+}$.[17] The Fe−Cl distances of 2.278, 2.293, and 2.311 Å are also close to the values generally observed for high spin Fe(III) complexes[18−21] and close to

(16) Simaan, A. J.; Poussereau, S.; Blondin, G.; Girerd, J. J.; Defaye, D.; Philouze, C.; Guilhem, J.; Tchertanov, L. *Inorg. Chim. Acta* **2000**, *299*, 221−230.

(17) Duelund, L.; Hazell, R.; McKenzie, C. J.; Nielsen, L. P.; Toftlund, H. *J. Chem. Soc., Dalton Trans.* **2001**, 152−156.

(18) Hazell, A.; Jensen, K. B.; McKenzie, C. J.; Toftlund, H. *Inorg. Chem.* **1994**, *33*, 3127.

(19) Arulsamy, N.; Hodgson, D. J.; Glerup, J. *Inorg. Chim. Acta* **1993**, *209*, 61.

(20) Nivorozhkin, A.; Anxolabéhère-Mallart, E.; Mialane, P.; Davydov, R.; Guilhem, J.; Cesario, M.; Audière, J.-P.; Girerd, J.-J.; Styring, S.; Schussler, L.; Seris, J.-L. *Inorg. Chem.* **1997**, *36*, 846.

(21) Raffard, N.; Carina, R.; Simaan, A. J.; Sainton, J.; Rivière, E.; Tchertanov, L.; Bourcier, S.; Bouchoux, G.; Delroisse, M.; Banse, F.; Girerd, J.-J. *Eur. J. Inorg. Chem.* **2001**, 2249−2254.

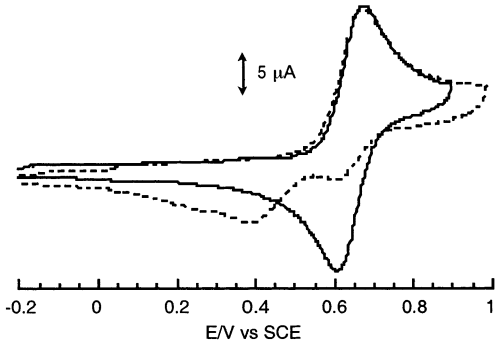

Figure 3. Cyclic voltammogram of $[L_5{}^3Fe^{II}Cl]^+$ (**1**) in acetonitrile (—) and in methanol (- - -) at 298 K. Concentration 1 mM, 100 mV/s scan rate.

those obtained for other Fe(III) complexes with three chloro ligands.[22] The angles around Fe are close to 90° except those belonging to a five-membered metallocycle (around 77°).

Electronic Spectroscopy. For complex **1**, the spectrum in methanol is dominated by a band at 383 nm with an extinction coefficient of 1290 M^{-1} cm^{-1}. This band is assigned to an Fe^{II}-to-pyridine charge transfer transition. Its intensity is consistent with a high spin state for the Fe^{II} ion.[10] The other band at 258 nm (8000 M^{-1} cm^{-1}) is due to a pyridine $\pi-\pi^*$ transition. For complex **2**, the spectrum in acetonitrile exhibits three bands at 388 nm (4200 M^{-1} cm^{-1}), 295 nm (6900 M^{-1} cm^{-1}), and 255 nm (15 700 M^{-1} cm^{-1}). The two first bands are tentatively assigned to chloro-to-Fe^{III} charge transfer transitions by analogy with a pure sample of $[FeCl_4]^-$ prepared as a reference compound for electrochemistry (see later), whereas the band in the UV is characteristic of $\pi-\pi^*$ transitions.

Electrochemistry of 1. As illustrated in Figure 3, cyclic voltammetry of **1** presents a quasireversible one-electron wave in acetonitrile ($\Delta E_p = 70$ mV). The half-wave potential value is 640 mV versus SCE for the oxidation of Fe^{II} to Fe^{III}. This value is about 70 mV higher than the one reported for the Fe^{II}/Fe^{III} couple with the closely related ligand L_5 ($E_{1/2} = 570$ mV vs SCE).[9] The comparison between both potentials is consistent with a greater stabilization of Fe^{II} with $L_5{}^3$ ligand. Moreover, in the case of $[L_5Fe^{III}Cl]^+$, an additional wave (25 mV) is observed on the reverse scan. The authors suggested that this additional wave could indicate a rapid rearrangement of Fe^{III} species generated at the electrode. Such an evolution of the Fe^{III} species is not observed with $L_5{}^3$ in acetonitrile. This may be due to the increased flexibility of the ligand $L_5{}^3$ compared to the related ligand L_5, leading to a less labile Fe^{III} complex.

The cyclic voltammogram of **1** was also recorded in methanol (Figure 3). No solvent effect was detected on the position of the oxidation peak, but reversibility of the oxidation wave is lost. On the reverse scan, in addition to the small wave at 605 mV corresponding to the reduction of $[L_5{}^3Fe^{III}Cl]^{2+}$ generated at the electrode, two other waves are observed at 385 and 240 mV. These two additional waves indicate that $[L_5{}^3Fe^{III}Cl]^{2+}$ is unstable in methanolic solution and rapidly (in less than 5 s) evolves to more stable species.

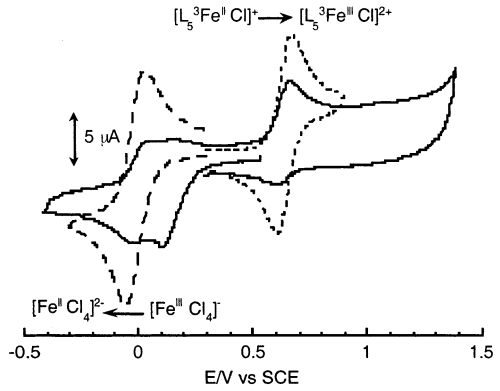

Figure 4. Cyclic voltammogram of $[(L_5{}^3H^+)Fe^{III}Cl_3]PF_6$ (**2**) in acetonitrile. Concentration 1 mM, 100 mV/s scan rate, 298 K. **2** (—), **1** (- - -), $[FeCl_4]^-$ (— — —).

We propose that these species are $[L_5{}^3Fe^{III}(OMe)]^{2+}$ and $[L_5{}^3Fe^{III}(OH)]^{2+}$. Indeed, the wave at 240 mV increased in intensity when water was added and is therefore attributed to $[L_5{}^3Fe^{III}(OH)]^{2+}$. The wave at 385 mV is assigned to $[L_5{}^3Fe^{III}(OMe)]^{2+}$. Recently, Goldsmith et al. reported the value of 488 mV for the reduction of $[Fe^{III}(PY5)(OMe)]^{2+}$.[23] The difference in the values of Goldsmith and ours is consistent owing to the greater number of pyridines in PY5 than in $L_5{}^3$. Similar $Fe^{III}(OMe)$ species have been reported with the pentadentate ligand N4Py.[24] Recently, these species have also been generated and characterized in solution with ligands of the L_5 series.[17] All these observations demonstrate that the ferric-methoxide and ferric-hydroxide complexes are easily obtained with pentadentate amine/pyridine ligands.

Electrochemistry of 2. Cyclic voltammetry of complex **2** in acetonitrile shows two reduction peaks at 75 and −40 mV (Figure 4). The first reduction peak at 75 mV is attributed to reduction of $[(L_5{}^3H^+)Fe^{III}Cl_3]^+$ and occurs at a lower potential than the one reported for $[(bpy)_2Fe^{III}Cl_2]^+$,[25] owing to the additional coordinated chloride. Thus, the electrochemical signature implies that the structure of **2**, with three-coordinated chlorides, is maintained in solution. This is also confirmed by the absence of any oxidation peak when scanning the potential up to 1.2 V where free chloride ions may be detected.

The second reduction peak (−40 mV) is reversible with $E_{1/2}$ at −20 mV. This second wave corresponds to the reversible wave of $[FeCl_4]^-$. The relative intensity of the two cathodic peaks depends on the potential scan rate, which indicates that $[FeCl_4]^-$ is generated from a fast chemical reaction coupled to the initial electron transfer. This fast rearrangement is responsible for the irreversibility observed for the reduction of **2**. Such a process has also been observed with $[(bpy)_2Fe^{III}Cl_2]^+$.[25] Moreover, EPR as well as electronic spectra indicate that $[FeCl_4]^-$ is not present in acetonitrile solution of **2**.

(22) Silver, G. C.; Trogler, W. C. *J. Am. Chem. Soc.* **1995**, *117*, 3983.

(23) Goldsmith, C. R.; Jonas, R. T.; Stack, T. D. P. *J. Am. Chem. Soc.* **2002**, *124*, 83−96.

(24) Roelfes, G.; Lubben, M.; Chen, K.; Ho, R. Y. N.; Meestma, A.; Genseberger, S.; Hermant, R. M.; Hage, R.; Mandal, S. K.; Young, V. G.; Zang, Y.; Kooijman, H.; Spek, A. L.; Que, L.; Feringa, B. L. *Inorg. Chem.* **1999**, *38*, 1929−1936.

(25) Collomb, M. N.; Deronzier, A.; Gorgy, K.; Leprêtre, J. C.; Pécaut, J. *New. J. Chem.* **1999**, 785.

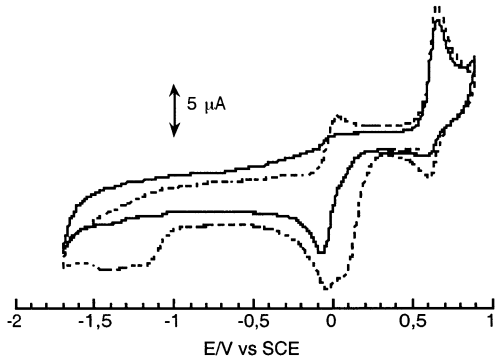

Figure 5. Cyclic voltammogram of $[(L_5^3H^+)Fe^{III}Cl_3]PF_6$ (**2**) in acetonitrile. Concentration 1 mM, 100 mV/s scan rate, 298 K. Before (- - -) and after (—) addition of 1 equiv of NEt_3.

As observed in Figure 4, an additional anodic peak is observed at 670 mV on the reverse scan. This anodic peak is accompanied by the appearance of the related cathodic peak at 605 mV ($E_{1/2} = 640$ mV), characteristic of complex **1**. This clearly demonstrates that, upon reduction, complex **2** is not stable and reorganizes itself to form complex **1** and $[FeCl_4]^-$. In addition, two peaks are observed at −1.2 and −1.4 V when scanning the solution toward negative potentials down to −2 V (cf. Figure 5). These potentials correspond to the reduction of protonated ligand resulting from the formation of $[FeCl_4]^-$.

In order to check these hypotheses, we recorded a voltammogram scanning from the Fe^{II} state. Two anodic peaks at 35 and 670 mV were observed in a 1:2 ratio independent of the scan rate, indicating that the reduction of **2** led to $FeCl_4^-$ and **1** in a 1:2 ratio.

Scheme 1 summarizes the overall process involved in the reduction of complex **2**.

From the careful analysis of the voltammogram in Figure 4, two more observations can be made. Even though chloride anions are released during the reduction process of **2**, their oxidation wave is not observed when scanning back to 1.2 V. At the same time, the anodic wave observed at 670 mV and attributed to the oxidation of $[L_5^3Fe^{II}Cl]^+$ is not reversible, contrary to what is observed when probing a solution of complex **1** (cf. Figure 3). These two observations are consistent with the fact that, in the presence of free Cl^-, L_5^3-Fe^{III} species readily coordinate free Cl^-, thus probably regenerating complex **2**.

Detection of a New Complex by Electrochemistry. Cyclic voltammetry of a solution of **2** is modified upon addition of 1 equiv of triethylamine, as shown in Figure 5. Only one irreversible peak is observed in reduction at −70 mV, and simultaneously, the reduction waves associated with the protonated ligand (at approximately −1.4 V in Figure 5, dashed line) disappear. On the reverse scan (oxidation), a peak is observed at 670 mV corresponding to the oxidation of complex **1**. A second quasireversible peak appears at 1.2 V (not shown) and is also observed when probing the solution toward oxidative potential. It corresponds to free chloride ions released consecutively to the addition of base. When comparing with cyclic voltammetry of a solution of known concentration, the intensity of the peak at 1.2 V indicates that 3 equiv of chloride are in solution. As explained in the previous section, these free chlorides are responsible for the irreversibility observed here for complex **1**.

The reduction potential observed at −70 mV can be attributed to an unsymmetrical dinuclear species $[L_5^3Fe^{III}$-$OFe^{III}Cl_3]^+$, **3**. It should be compared to the value of −25 mV reported for $[N5FeOFeCl_3]^+$.[26] The difference in potential may be related to a better stabilization of the Fe^{II} with the poly-benzimidazol ligand N5 and also to the fact that our L_5^3 ligand is less bulky.[16] No second reduction wave is observed even at higher scan rates, indicating that the mixed valence species formed after the initial electron transfer is not stable under those conditions. The observation of the anodic wave at 670 mV on the reverse scan indicates that one of the generated species is the mononuclear $[L_5^3Fe^{II}$-$Cl]^+$ species.

In parallel to these experiments, an aliquot of the solution has been studied by EPR. Its spectrum shows a significant extinction of the high spin Fe^{III} resonance related to **2**. The above-mentioned observations are consistent with the formation of a dinuclear EPR-silent species. The hypothesis of an unsymmetrical diiron(III) species is supported by UV−vis and EI-MS. As shown in Figure 6, the UV−vis spectrum in acetonitrile for the electrochemical solution obtained after addition of base exhibits four bands at 514 nm (120 M^{-1} cm^{-1}), 400 nm (1600 M^{-1} cm^{-1}), 338 nm (7300 M^{-1} cm^{-1}), and 255 nm (15 800 M^{-1} cm^{-1}). The energy as well as the low intensity of the band at 514 nm is indicative of an Fe^{III}−O−Fe^{III} unit in a quite linear geometry.[27] The other features are reminiscent of the electronic spectra of the unsymmetrical dinuclear complexes $[N5FeOFeCl_3]^+$ [26] and $[L_4^3Fe^{III}(Cl)(\mu$-$O)Fe^{III}Cl_3]$[28] (L_4^3 being *N*,*N*′-dimethyl-*N*,*N*′-bis(2-pyridylmethyl)propane-1,3-diamine, the tetradentate analogue of L_5^3). The band at 255 nm is due to $\pi-\pi^*$ transitions of the ligand, and the transitions at 338 and 400 nm are assigned as Cl^--to-Fe(III) and oxo-to-Fe(III) charge transfer transitions, respectively.[26,29]

Until now, attempts to isolate the pure compound $[L_5^3$-$Fe^{III}OFe^{III}Cl_3]^+$ as a solid have been unsuccessful. However, the isolated powder has been characterized by different techniques. Its UV−vis spectrum is identical to the one represented in Figure 6. Moreover, the EI-MS spectrum of this powder in acetonitrile has allowed us to detect this unsymmetrical dinuclear complex (see Supporting Information). As a matter of fact, the following structure (Scheme 2) can be proposed for the dinuclear species **3** generated in solution by addition of base to complex **2**.

Reactivity of 1 with H_2O_2. The reaction of a methanol solution of complex **1** with 100 equiv of H_2O_2 led to the formation of a purple species that was characterized by UV−vis at −40 °C, EPR, and resonance Raman spectroscopies. The spectroscopic data are presented in Table 3.

(26) Gómez-Romero, P.; Witten, E. H.; Reiff, W. M.; Backes, G.; Sanders-Loehr, J.; Jameson, G. B. *J. Am. Chem. Soc.* **1989**, *111*, 9039.
(27) Zheng, H.; Zang, Y.; Dong, Y.; Young, V. G.; Que, L. *J. Am. Chem. Soc.* **1999**, *121*, 2226.
(28) Raffard, N. Thèse de Doctorat, Université Paris XI, Orsay, 2002.
(29) Wang, J.; Mashuta, M. S.; Sun, Z.; Richardson, J. F.; Hendrickson, D. N.; Buchanan, R. M. *Inorg. Chem.* **1996**, *35*, 6642.

Scheme 1. Process Involved in the Reduction of Complex **2**

$$3\,[(L_5{}^3H^+)Fe^{III}Cl_3]^+ + 2\,e^- \rightarrow [Fe^{III}Cl_4]^- + 2\,[L_5{}^3Fe^{II}Cl]^+ + 3\,H^+ + 3\,Cl^- + L_5{}^3$$

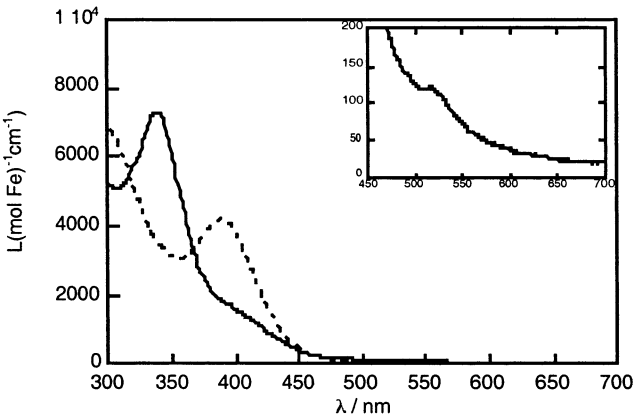

Figure 6. UV−vis spectra of $[(L_5{}^3H^+)Fe^{III}Cl_3]PF_6$ (**2**) in acetonitrile. Before (- - -) and after (—) addition of base. The extinction coefficients are given as L (mol Fe)$^{-1}$ cm^{-1}.

Scheme 2. Structure Proposed for the Dinuclear Complex **3**

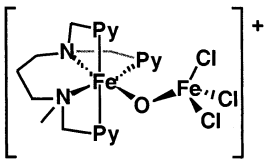

Table 3. Spectroscopic Characterization of the Hydroperoxo Intermediates Obtained with Several Aminopyridine Ligands

ligand	λ_{max} (M^{-1} cm^{-1})	*g* values	ν_{Fe-O} (cm^{-1})	ν_{O-O} (cm^{-1})	ref
$L_5{}^3$	550 (571)	1.92, 2.1, 2.155	609	799	this work
L_5	537 (1000)	1.95, 2.12, 2.19	617.2	796.4	31
TPEN	541 (900)	1.967, 2.15, 2.22	617.2	795.9	31
N4Py	548 (1100)	1.98, 2.12, 2.17	632	790	24

The purple species is characterized by an absorption band at 550 nm ($\epsilon_{observed} = 571$ M^{-1} cm^{-1}). This complex rapidly decomposes as testified by the disappearance of the band at 550 nm. By comparison with numerous models reported in the literature, this band is assigned as an LMCT between the hydroperoxo group and the Fe^{III} for a low spin Fe−OOH entity.[1,30] The extinction coefficient value is low compared to other Fe−OOH compounds with similar ligands.[9,10,31] Given that the ϵ value is generally about 1000 M^{-1} cm^{-1}, it is likely that the purple complex reported here is obtained in ca. 60% yield only. The low yield observed may be related to the short lifetime of the Fe−OOH complex.

The EPR spectrum of this intermediate is typical of a low spin Fe^{III} in a quite axial symmetry with *g* values of 2.155, 2.1, and 1.92. This spectrum is similar to those usually observed for other hydroperoxo complexes (see Table 3).[1,13,14] The analysis of the *g* values by using the model of Griffith[32]

Scheme 3. Structure of $[L_5{}^3FeOOH]^{2+}$

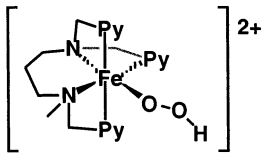

as presented by Taylor[33] leads to an estimation of the rhombic distortion energy *V* and of the axial energy Δ. In units of the spin-coupling parameter λ, we obtain $(V/\lambda) = 3.04$ and $(\Delta/\lambda) = -10.9$. These results are in agreement with what has been obtained for low spin Fe−OOH entities prepared with ligands containing 3 pyridines.[1] Other signals are observed at $g = 2.34$ and $g = 1.88$, corresponding to the g_{max} and g_{min} resonances of a LS (low spin) rhombic mononuclear Fe(III). This latter complex can be assigned as $[L_5{}^3FeX]^{2+}$, with X = Cl^-, OH^-, or MeO^-.[10,17,34]

The Fe−O and O−O vibrational frequencies have been obtained by performing resonance Raman studies of the purple species. From these values (see Table 3), it is notable that the Fe−O frequency thus obtained (609 cm^{-1}) is similar but lower than the analogous frequency reported for low spin Fe−OOH models with similar ligands.[1] Moreover, the O−O vibrational frequency is relatively high. These observations are consistent with Raman data reported for other low spin Fe−OOH entities.[1] Indeed, the general tendency is that the Fe−O frequency increases when the O−O frequency decreases.

Taken together, the described observations obtained for the compound resulting from the reaction of **1** with H_2O_2 permit us to propose it as $[L_5{}^3FeOOH]^{2+}$ with the structural configuration represented in Scheme 3.

Kinetic Study of the Formation and Degradation of $[L_5{}^3FeOOH]^{2+}$. The reaction of **1** with 100 equiv of H_2O_2 in MeOH has been followed by stopped-flow at $T = 20$, 15, 10, and 5 °C. The evolution versus time of the intensity of the LMCT band at 540 nm is shown in Figure 7. Each set of experimental data displays the same kind of evolution: in a first step, the intensity increases revealing the formation of the purple complex, and then it reaches a maximum and finally decreases during a slower step reflecting the degradation of the Fe−OOH species. To reproduce these data by an analytical expression, we propose the following mechanism for the formation and degradation of the purple complex (Scheme 4).

However, some simplifying assumptions have been applied. (i) Complex **1** is rapidly oxidized by H_2O_2 to give $[L_5{}^3Fe^{III}Cl]^{2+}$. This latter complex rearranges to give $[L_5{}^3Fe^{III}(OH)]^{2+}$ with $K \gg 1$. This last proposition is supported by the characterization of **1** by electrochemistry (see earlier) and the EPR studies of methanol solutions of $[Fe^{III}(bztpen)Cl](PF_6)_2$ and $[Fe^{III}(bztpen)Cl](ClO_4)_2$ reported by Hazell et

(30) Solomon, E. I.; Brunold, T. C.; Davis, M. I.; Kemsley, J. N.; Lee, S.-K.; Lehnert, N.; Neese, F.; Skulan, A. J.; Yang, Y.-S.; Zhou, J. *Chem. Rev.* **2000**, *100*, 235−349.
(31) Simaan, A. J.; Döpner, S.; Banse, F.; Bourcier, S.; Bouchoux, G.; Boussac, A.; Hildebrandt, P.; Girerd, J. J. *Eur. J. Inorg. Chem.* **2000**, 1627−1633.
(32) Griffith, J. S. *The theory of transition metal ions*; Cambridge University Press: London, 1961.
(33) Taylor, C. P. S. *Biochim. Biophys. Acta* **1977**, *491*, 137−149.
(34) Lippai, I.; Magliozzo, R. S.; Peisach, J. *J. Am. Chem. Soc.* **1999**, *121*, 780−784.

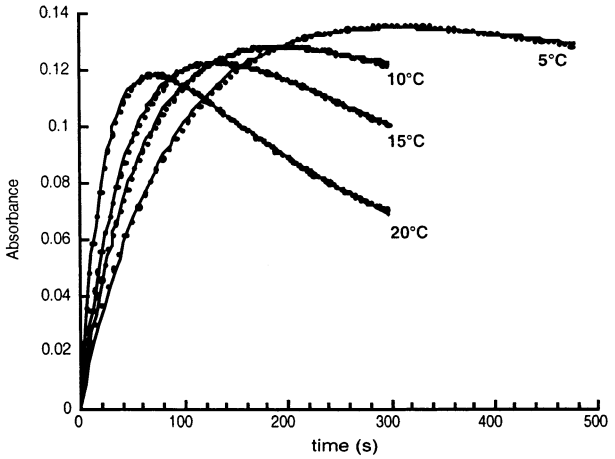

Figure 7. Evolution vs time of the intensity of the hydroperoxo-to-Fe^{III} charge transfer absorption band monitored at 550 nm. The double exponential fit is superimposing the experimental points.

Scheme 4. Mechanism Proposed for the Formation and Degradation of $[L_5{}^3FeOOH]^{2+}$

$$Fe^{II}\text{-}Cl \longrightarrow Fe^{III}\text{-}Cl \overset{K}{\rightleftharpoons} Fe^{III}\text{-}OH$$

$$Fe^{III}\text{-}OH + H_2O_2 \underset{k_{-1}}{\overset{k_1}{\rightleftharpoons}} Fe^{III}\text{-}OOH \xrightarrow{k_2} \text{products}$$

Scheme 5. Analytical Law Used to Reproduce the Formation and Degradation of $[L_5{}^3Fe^{III}OOH]^{2+}$ as a Function of Time[a]

$$\left[[L_5{}^3Fe^{III}OOH]^{2+}\right] = \frac{(C_0 \times k_1')}{(k_2 - k_1')}\left[e^{-k_1't} - e^{-k_2t}\right]$$

[a] C_0 is the initial concentration in **1**, and $k'_1 = k_1[H_2O_2]$.

Scheme 6. Eyring Relationship

$$\ln\frac{k}{T} = -\frac{\Delta H^{\#}}{RT} + \frac{\Delta S^{\#}}{R} + 23.8$$

al. which showed that the chloride ion was substituted by solvent.[14] (ii) By using a large excess of hydrogen peroxide, the back reaction of the formation of $[L_5{}^3Fe^{III}OOH]^{2+}$ is negligible.[14] For the same reason, we can consider a pseudo-first-order rate for the formation of $[L_5{}^3Fe^{III}OOH]^{2+}$. We finally obtain a classical A → B → C mechanism with A, B, and C being $[L_5{}^3Fe^{III}(OH)]^{2+}$, $[L_5{}^3Fe^{III}OOH]^{2+}$, and the degradation products, respectively. The concentration of $[L_5{}^3Fe^{III}OOH]^{2+}$ is then given by the expression in Scheme 5.[35]This expression allows us to obtain satisfactory fits as seen in Figure 7.

The values so obtained for k_1 and k_2 have been used to calculate the activation parameters $\Delta H^{\ddagger}$ and $\Delta S^{\ddagger}$ for both formation and degradation reactions by using the Eyring relationship (Scheme 6).[35]

All the rate constants and activation parameters are reported in Table 4. At 20 and 10 °C, the rate constants k_1 obtained by Hazell and co-workers for the reaction of $[Fe^{III}(bztpen)Cl](ClO_4)_2$ with 500 equiv of hydrogen peroxide are 0.35 and 0.160 M^{-1} s^{-1}, respectively.[14] The values found by us or by Hazell et al. are of the same order, confirming

(35) Wilkins, R. G. *Kinetics and Mechanism of Reactions of Transition Metal Complexes*; VCH: Weinheim, 1991.

Table 4. Rate Constants and Activation Parameters for the Formation and Degradation of $[L_5{}^3Fe^{III}OOH]^{2+}$[a]

T (°C)	k_1 (M^{-1} s^{-1})	$\Delta H^{\ddagger}_1$ (kJ mol^{-1})	$\Delta S^{\ddagger}_1$ (J mol^{-1} K^{-1})	k_2 (s^{-1})	$\Delta H^{\ddagger}_2$ (kJ mol^{-1})	$\Delta S^{\ddagger}_2$ (J mol^{-1} K^{-1})
5	0.222			0.0004		
10	0.336 (0.16)	53 (53)	−66 (−72)	0.0007	84	−9
15	0.426			0.0016		
20	0.808 (0.35)			0.0027		

[a] Data in brackets are from ref 14.

the validity of the mechanism already described. As a consequence, the enthalpy of activation $\Delta H^{\ddagger}_1$ obtained for the formation of the purple species is the same for both systems, and the values of entropy of activation $\Delta S^{\ddagger}_1$ are similar for both systems (see Table 4). Since $\Delta S^{\ddagger}_1$ is negative, it is very likely that the mechanism is associative in character. It appears that the rate and mechanism of formation of the Fe−OOH species are independent of the substituent borne by the ligand and of the length of the spacer between the amino functions.

For the degradation of Fe−OOH complexes obtained with similar ligands, no kinetic data have been reported to date, as they are generally stable for a long time. In the present case, the hydroperoxo adduct is quite unstable, and the rate constants k_2 extracted from fits are listed in Table 4. The relative instability of the purple complex might be related to the enhanced flexibility of the ligand. Recently, Mekmouche et al. have studied the kinetics of the reaction between a substrate and a hydroperoxoiron complex, formulated as $[Fe(OOH)(pb)_2]^{2+}$ where pb designates the bidentate ligand 4,5-pinene-2,2′-bipyridine.[36] At 0 °C and without substrate, they obtained a rate constant for the degradation of $[Fe(OOH)(pb)_2]^{2+}$ of ca. 2×10^{-3} s^{-1}. At 5 °C, we obtained $k_2 = 4 \times 10^{-4}$ s^{-1} (see Table 4). From this comparison, it is clear that the Fe−OOH complex is much more stabilized by a pentadentate ligand than by bidentate ones. The activation parameters obtained from a Eyring plot are $\Delta H^{\ddagger}_2 = 84$ kJ mol^{-1} and $\Delta S^{\ddagger}_2 = -9$ J mol^{-1} K^{-1}. This large activation enthalpy and weakly negative activation entropy are probably reflecting a mechanism with an associative character weaker than that of the formation of the hydroperoxo complex, although it is difficult to propose a mechanism from only one set of values.

Conclusion

Two new complexes are reported with the amine/pyridine ligand $L_5{}^3$. The Fe^{II} compound $[L_5{}^3FeCl]^+$ exhibits a structure that is similar to the one reported for complexes with similar ligands.[10,14] On the contrary, the Fe^{III} complex $[(L_5{}^3H^+)Fe^{III}Cl_3]^+$ has an unusual structure with only three nitrogen atoms of the ligand bound to the metal center and three chloride ions to complete the coordination sphere. When treated with a base, this last compound converts to an unsymmetrical dinuclear ferric complex as revealed by the solution studies.

(36) Mekmouche, Y.; Hummel, H.; Ho, R. Y. N.; Que, L.; Schunemann, V.; Thomas, F.; Trautwein, A. X.; Lebrun, C.; Gorgy, K.; Lepretre, J. C.; Collomb, M. N.; Deronzier, A.; Fontecave, M.; Menage, S. *Chem. Eur. J.* **2002**, *8*, 1196−1204.

With a 1,3-diaminopropane-containing tetradendate ligand, we prepared recently another unsymmetrical dinuclear Fe(III) complex able to catalyze the oxidation of hexane into hexanols by dioxygen in the presence of a hydroquinone as electron donor.[37,38] The L_5^3 ligand with the C_3 chain between the amino functions adopts then different manners to accommodate the small radius Fe^{III} ion. This versatility in coordination does not seem to occur with the larger Fe^{II} ion. The reaction of $[L_5^3FeCl]^+$ with hydrogen peroxide allows the observation of the low spin hydroperoxo ferric motif $[L_5^3FeOOH]^{2+}$, but the latter is much less stable than the one with L_5.[14] This nevertheless adds a new example to the family of non-heme Fe−OOH species that came to light during the last years owing to chemists' efforts. The Fe−O vibrational frequency of $[L_5^3FeOOH]^{2+}$ is lower than what has been previously reported for analogous complexes. Reactivity studies need now to be completed with $[L_5^3FeOOH]^{2+}$ and $[L_5FeOOH]^{2+}$ in order to understand if the relative stability of these complexes is related to their reactivity.

Acknowledgment. The authors thank Félix Pérez, Laboratoire de Chimie Structurale Organique, UPRESA 8074, for his assistance in EI-MS experiments.

Supporting Information Available: Figure S1 displaying the electrospray-ionization mass spectrometric feature of $[L_5^3Fe^{III}OFe^{III}Cl_3]^+$ (**3**) at *m*/*z* 594. Figure S2 representing the theoretical isotope patterns for the same complex. This material is available free of charge via the Internet at http://pubs.acs.org.

IC025905N

(37) Raffard, N.; Balland, V.; Simaan, J.; Létard, S.; Nierlich, M.; Miki, K.; Banse, F.; Anxolabehere-Mallart, E.; Girerd, J.-J. *C. R. Chim.* **2002**, *5*, 99−109.
(38) Raffard, N.; Banse, F.; Miki, K.; Nierlich, M.; Girerd, J.-J. *Eur. J. Inorg. Chem.* **2002**, 1941−1944.